ACCELERATING STRUCTURES FOR SUPERCONDUCTING ELECTRON LINACS*

J.N. Weaver, T.I. Smith, and P.B. Wilson
High Energy Physics Laboratory
Stanford University
Stanford, California

Summary

A study to determine the optimum slow wave structure for a superconducting linear accelerator is being conducted. Vacuum, thermal, and mechanical problems at cryogenic temperatures impose limitations on such structures. Ultimately, the maximum energy gradient in a superconducting structure is limited by the critical magnetic field or electric field breakdown. At present a $\pi/2$, bi-periodic, standing-wave structure is favored. Calculations of the dispersion diagram and longitudinal electric field profile has been obtained from a coupled resonator, normal mode analysis. A comparison is made with room temperature measurements on stacked test cells. The effects of full end cells and of incorrectly tuned cells on the flatness of the electric field profile are considered. The relationship between cell tuning and the presence of a stop band in the dispersion curve is shown. Problems of coupling to a high Q superconducting structure and tuning the frequencies of sections in a multi-section linac are considered. Results are given for the Q, the dispersion diagram, and the energy gain for a 952 MHz lead-plated superconducting structure 5 feet in length operating near $2^{\circ}K$.

I. Introduction

The principles underlying the design and measurement of slow wave structures suitable for use in a superconducting electron linac have many points in common with the design and measurement of room temperature structures. There are, however important differences. The cryogenic environment is an obvious factor which must be considered in the case of a superconducting structure. Other factors, such as susceptibility to beam break-up, may be less obvious. These and other design criteria for such structures are considered in the next section. It will be shown that a $\pi/2$ mode bi-periodic, disk loaded structure meets many of the requirements for an efficient accelerator. Some results of a theoretical analysis of a structure of this type are presented briefly in section III. In section IV measurements of the dispersion curve, field profile, and shunt impedance are discussed, and examples given for two bi-periodic structures, one 5 feet long and one $1\frac{1}{2}$ feet long operating at 952 MHz. Results obtained during low temperature operation are presented.

II. Design Criteria for Superconducting Structures

The Q of a superconducting accelerator can be expected to be on the order of 10^5 times that of a conventional accelerator. It is impractical to increase the physical length or decrease the group velocity of a traveling wave structure by this large factor to maintain the attenuation length close to unity. A superconducting accelerator section must then be operated as part of a resonant ring or as a standing wave cavity. The complexity of a cryogenic ring eliminates this device from serious consideration at present.

In any accelerating structure it is desirable to make the shunt impedance as large as possible. However, some shunt impedance may have to be sacrificed in order to satisfy other criteria. Specifically, the existence of a critical magnetic field and a limiting electric field must be taken into account. Measurements[1] have shown that the rf critical magnetic field is about equal to the dc critical field at microwave frequencies. In a typical lead-plated standing wave structure this will limit the energy gradient to about 5 Mev per foot. The limit will be two to three times this value in a niobium structure.

At present electric field break down imposes a more severe limit on the energy gradient. Limits on the electric field strength arise from several sources. At relatively low fields multipactoring can occur. The problem of suppressing multipactoring in a superconducting structure seems to be similar to the problem in conventional structures. Materials with a low coefficient of secondary electron emission are desired, and structures with closely spaced parallel surfaces should be avoided. Fortunately, lead is favorable in the first respect, having a secondary emission coefficient $\delta = 1.1$. The importance of this coefficient is shown by the fact that some structures when lead plated did not multipactor, but showed evidence of severe multipactor when plated with tin ($\delta = 1.35$). In this respect niobium, with $\delta = 1.2$, is intermediate. The fact that closely spaced parallel surfaces should be avoided implies that a superconducting structure should be terminated in full end cavities.

At relatively high electric field strengths many cavities tested so far have shown evidence of electron loading. The probable source of the loading is field emission current from sharp "whiskers" on the cavity surface. This field emission current serves as a mechanism for converting rf power into heat dissipated at the low temperature. The power dissipation from this source becomes intolerable when a level of about one watt per foot is reached. Since the field emission current increases exponentially with increasing field strength, a fairly rigid limit is imposed on the peak field strength E_p existing anywhere on the surface of the structure. To obtain the highest average energy gradient $\bar{E}$ it is therefore desirable to optimize the ratio $\bar{E}/E_p$ for the structure. This favors the choice of a structure without nose cones on the loading discs. Although nose cones do significantly raise the shunt impedance of a structure, calculations done at Los Alamos[2] have shown that a 10% increase in the shunt impedance is accompanied by a doubling of the peak

* Work supported in part by the U.S. Office of Naval Research, Contract [Nonr 225(67)].

electric field at the surface.

Fabrication and electroplating considerations have a bearing on the choice of structure. Electroplating is facilitated if the inside corners of the cavities are well rounded, if the beam aperature is large enough to insert bagged plating anodes, and if the disks are tapered to facilitate the escape of gas bubbles during electroplating and the drainage of the various cleaning, plating and rinsing baths. It is convenient to be able to plate the individual cells separately, and then stack them together using indium gaskets to form a completed section. The $\pi/2$ mode, in which alternate cells are not excited and the indium joints can be made in a region of zero current, is thus indicated.

Since the unexcited cells in the standing wave $\pi/2$ mode do not contribute to acceleration, the shunt impedance can be improved by placing these cells off to the side (e.g. the Los Alamos side-coupled structure) or by shortening the length of these cells in a disk loaded structure. We have chosen this latter alternative since it is simple to fabricate and electroplate.

Several cryogenic problems must be considered in the design of a structure. The geometry must be chosen such that thermal impedance into the helium bath is low from all surfaces where power is dissipated. For example, it would not be desirable to have magnetic coupling holes that take up a large fraction of the circumference of a loading disk, thereby blocking the flow of heat from the inner portions of the disk. The body of the structure must of course be made of material with a high thermal conductivity at liquid helium temperatures such as OFHC copper or high purity aluminum. In addition since operation below the lambda point is planned, all joints and gaskets must be well designed and vacuum tight to prevent superfluid helium leaks.

In a multi-section linac, the frequences of the sections must be matched to about one part in 10^9. Since this cannot be accomplished by pretuning at room temperature, an adjustable tuner capable of pulling the frequency of the structure by about one part in 10^5 while at helium temperatures is needed. Calculations have shown[5] that for the $\pi/2$ mode this can be accomplished by tuning a single cavity of the structure, without serious distortion of the field profile.

It will also be desirable to adjust the coupling to the cavity in order to allow efficient operation over a wide range of beam current. There are many possible mechanisms for accomplishing this, such as the system of three matching plunger shown in Fig. 1 for the Stanford 5-foot linac. However, a variable length section of waveguide below cut-off seems more attractive. The length of the cut-off section could be varied using a moveable dielectric rod, or by making the cut-off section out of a bellows using a moveable dielectric.

An effort must be made in the design of a superconducting linac structure to supress the excitation of the transverse deflection modes which can lead to beam break-up. One way to accomplish this is to adjust the length and diameter of the beam coupling holes at each end of an accelerator section so that the holes are below cut-off and have sufficient attenuation to contain the fundamental accelerating mode, but yet will propagate power in the higher order deflection modes out of the section.

Two types of beam break-up must be considered, the type of break-up in which a single section can act as an oscillator with internal feedback, and the type observed more recently in long, multi-section linacs. Helm[3] has calculated that for this latter kind of break-up the Q for the deflecting modes must be less than 10^6 if a current of 1 ma is to be obtained in a 500 foot linac. The start-oscillation current for the former type of break-up can be estimated using a relation adapted from a calculation by Gluckstern[4].

$$I \approx \frac{1}{30}\frac{V_o \lambda^2}{L^2 Q}$$

Here V_o is the beam energy, L the section length, and $r/Q \approx 75/\lambda$ has been assumed for the first deflection mode. Using L = 300 cm, λ = 30 cm, V_o = 30 Mev and $Q = 10^5$, a break-up current of 3 ma obtained. In the case of a capture section, where the energy varies from a low value to the final energy of 30 Mev, a reduction in the break-up current by about a factor of 3 to I ≈ 1 ma can be expected. For either type of break-up it is evident that heavy loading of the higher order deflection modes is required.

III. Theory

A fairly good understanding of a standing wave structure can be obtained through the use of a model in which the cavities are assumed to be lumped resonant circuits, coupled to each other through their mutual inductances[5]. This model gives information only about the relative excitation of each cavity, which is assumed to be proportional to the current in the circuit representing the cavity, and says nothing about the spatial variation of the field within a cavity.

In spite of its limitations, the model has been very useful in studying such things as the effect of machining tolerances on the field profile of a structure, the effect of next nearest neighbor coupling, and the effect of a difference in frequency between the even and odd cavities in the bi-periodic structure.

When there is no next nearest neighbor coupling, and when all of the cavities have the same resonant frequency, the model is particularly simple. The normal modes calculated for a structure with full end cavities and for a structure with half end cavities are given below, for comparison with Fig. 4.

For the half cavity termination,

$$(\omega_o/\omega_q)^2 = 1+k\cos(\pi q/N) \qquad q = 0,1,2,\ldots,N \quad (1)$$

$$E_n^q = E_o \cos(n\pi q/N) \qquad n = 0,2,\ldots,N \quad (2)$$

$$E_n^q = E_o \sqrt{u_e/u_o}\cos(n\pi q/N) \qquad n = 1,3,\ldots,N \quad (2')$$

and for the full cavity termination,

$$(\omega_o/\omega_q)^2 = 1+k\cos(\pi q/N+1) \qquad q = 1,2,\ldots,N \quad (3)$$

$$E_n^q = E_o \sin(n\pi q/N+1) \qquad n = 1,3,\ldots,N \quad (4)$$

$$E_n^q = E_o \sqrt{u_o/u_e}\sin(n\pi q/N+1) \qquad n = 2,4,\ldots,N \quad (4')$$

In the above, ω_0 is the resonant frequency of an individual cavity, k is the coupling coefficient between cavities, E_n^q refers to the electric field in the nth cavity in the qth mode, and N is the number of full cavities in the structure. For a structure with a half cavity at each end, the total number of cavities is N+1. The coefficient $\sqrt{u_e/u_o}$ is the square root of the ratio of the energy in the even cavities to the energy in the odd cavities when the peak field in each cavity is the same. It reflects the fact that the energy distribution among cavities is unaffected in a particular mode by the shape of the cavities, as long as the frequency is constant. This behavior is particularly evident in the curve labeled '$\pi/20$ mode' in Fig. 4. For this curve Eqs. (4) apply with q = 1.

IV. Measurements

Microwave measurements were made, both at room temperature and at liquid helium temperatures, on the 19 cell structure shown schematically in Fig. 1. This structure, operating near 950 MHz, is the accelerating section for a five foot superconducting test linac. A block diagram of this accelerator is shown in Fig. 2. Detailed room temperature measurements were also made on a 5 cell structure to be used for Q and electric field breakdown tests.

Measurements were first made to determine the resonant frequency of each individual cell in the structure. The cells were fabricated from rings machined on a tracer lathe from copper forgings. Each ring consisted of half a short cell and half of a long cell with a loading disk between. The resonant frequency of each half cell was measured by clamping a shorting plate containing a magnetic coupling probe across one end of a ring, leaving the coupled half cell on the other side of the ring open to air. The resonant frequency could be measured in this manner to an accuracy of about 5×10^{-5}. This can be compared with the machining tolerance of about 6×10^{-5}. To obtain the resonant frequency of each full cell, the frequencies of the two component half cells were averaged. This proved to be more accurate than measuring the resonant frequency of the full cell directly because of the perturbation produced in attempting to couple to the electric field in the region of the coupling hole.

The resonant frequencies of the cells in the 19 cell structure were found to lie within a spread of 0.2 MHz. However, the average short cell frequency was 0.4 MHz lower than the average long cell frequency. This produced the 0.45 MHz gap in the dispersion curve, which is shown in Fig. 3. The five cell structure was machined more accurately; both long and short cells differed in frequency by less than 0.1 MHz.

It is interesting to examine the effect of this frequency error on the axial electric field profile and to compare these measurements with the theoretical results in section III. The field profile was determined in the usual way by pulling a dielectric bead through the structure. The estimated accuracy of the measurement of the electric field is $\pm$ 1% of the maximum value. For the 19 cell structure the fields in the excited cells were constant to within the accuracy of the measurement, except for the end cells which were 4% and 7% higher. The frequencies of the end cells were somewhat mistuned in this structure. The fields in the excited cells were under 5% of the excited cell level. If the long and short cells had been tuned to the same frequency, the analysis outlined in the preceeding section predicts a flatness of .001% for the excited cell field, and an unexcited cell field level of 2%. In the 5 cell structure the end cells were tuned more accurately and the field levels were measured to be 2% and 3% higher than the field in the center cell, while fields in the two unexcited cells were less than the accuracy of the measurement. A plot of the field profile is shown in Fig. 5 for the cases where the structure is terminated in full end cells and in half cavities. It is seen that the field profile looks very much like a sine wave (except in the end cells), indicating a fundamental space harmonic component close to unity. Note also that the electrical length of the structure terminated in full end cells is about $1\frac{1}{2}$ wavelengths, whereas the physical length is $1/6$ wavelength shorter. Thus the structure appears to be terminated in an "open" located at the center of phantom unexcited cells adjacent to the end cells.

This behavior is brought out more clearly in Fig. 4 where the field profiles or the $\pi/20$ and 19 $\pi/20$ modes are plotted for the 19 cell structure. Note that amplitude of the profile has a sine modulation, falling to zero at each end of the structure. This behavior is predicted by Eqs. (4) for the case of a structure terminated in full end cells. Note also that for the $\pi/20$ mode the fields in the short cells are greater than the fields in the long cells, as expected from Eq. (4').

Figure 3 shows the dispersion curve both at room temperature and at 4.2°K. The principle contribution to the frequency shift is the thermal contraction of copper. Equation (3) for the case of full end cells predicts that the slope of the dispersion curve should not be zero at the $\pi/20$ and 19 $\pi/20$ modes. This was measured experimentally as shown in Fig. 3. The same structure was measured with half end cells and in that case did show approximately a zero slope in the neighborhood of the 0 and π modes, as expected from Eq. (1).

The individual rings were assembled into a completed structure as illustrated in Fig. 1. Brazed joints were made in the center of each long cell. The resulting units, consisting of a long cell with half a short cell on either end, were electroplated and then stacked together with indium gaskets. The assembled structure was then placed in the dewar as indicated in Fig. 2 and cooled to liquid helium temperatures. Using the rf circuitry shown in the figure, the Q of the structure was measured by the decrement method at low power levels. An unloaded Q of 2.5×10^8 was obtained at 2°K.

The energy gain of a superconducting accelerator section can be written as

$$V = A\sqrt{(r/Q)LPQ}_o$$

where r is the shunt impedance per unit length, L is the length, and P the input power. The constant A is unity for relativistic electron energies. In a capture section, however, possible phase slip must be taken into account and A will be less than unity.

The shunt impedance can be obtained from a measured value of the unloaded Q and from the r/Q

ratio given by

$$\frac{r}{Q} = \left(\frac{a_o}{\Sigma a_n}\right)^2 \cdot \frac{60\lambda L}{K} \cdot \left(\frac{\delta\omega}{\omega}\right)$$

Here λ is the free space wave length, L the electrical length of the structure, and $\delta\omega/\omega$ the frequency perturbation when the perturbing bead is located at a field maximum where the space harmonics are summed. The ratio of the fundamental space harmonic component a_o to the sum Σa_n of all the harmonic components is obtained from a Fourier analysis of the field profile. The constant K is the effective volume of the bead and is obtained from the frequency shift for the bead in a TM_{010} calibration cavity of known dimensions. For the bi-periodic structure under measurement here a value of $(a_o/\Sigma a_n)^2 = .966$ was obtained. The r/Q was measured to be 920 ohms per meter, which is about 20% higher than expected from a singly periodic $\pi/2$ mode standing wave structure. A room temperature Q of 23,500 was obtained for the copper structure before lead plating.

Some of the properties of the higher order transverse modes were measured. The passband for the TM_{11}- like deflection mode extends from 1359MHz to 1436 MHz with a 46 MHz gap at the $\pi/2$ mode. The $v_p = c$ line crosses the dispersion curve for this mode at $\beta\ell = 0.72\pi$. At this point a non-zero v_g of -0.005c is obtained. Thus if selective loading can be provided at some point in the accelerator section for this mode, there would be no problem in suppressing the Q to provide protection against beam break-up. However, still higher order deflection modes must be carefully checked before the design of such a structure is considered final.

V. Conclusion

Initial tests have been made using the 19 cell structure as a five foot superconducting linac section. An electron beam was accelerated to an energy of 6 Mev. Taking account of phase slip during the capture process, an energy gradient of about 1.8 Mev per foot in the structure is indicated. This gradient is consistent with the observed input power and a Q of about 10^8 measured during operation at 2°K.

It is felt that by further work a considerably higher Q and a higher energy gradient will be obtained. A more thorough theoretical analysis of the bi-periodic structure is now being made, and further work is in progress to check the effect on shunt impedance and field profile of various parameters of the structure. Low temperature tests to measure the Q and electric field break down effects in suitable structures will continue.

References

1. J.P. Turneaure, "Microwave Measurements on the Surface Impedance of Superconducting Tin and Lead", Ph.D. thesis, Stanford University (1966).
2. H.C. Hoyt, private communication.
3. R. Helm, private communication.
4. R.L. Gluckstern, "Transverse Beam Blow-up in Standing Wave Linacs", Proceedings of the 1964 MURA Linear Accelerator Conference, p. 186.
5. T.I. Smith, to be published. See also "Standing Wave H Modes in a Superconducting Linear Accelerator", High Energy Physics Laboratory Report No. 437, Stanford University (April, 1966).

Acknowledgements

The mechanical design of the structure reported on here is largely due to H. Landsbergen. H. A. Schwettman participated in the design and analysis of the structure. The assistance of J. B. Styles in making the microwave measurements is acknowledged.

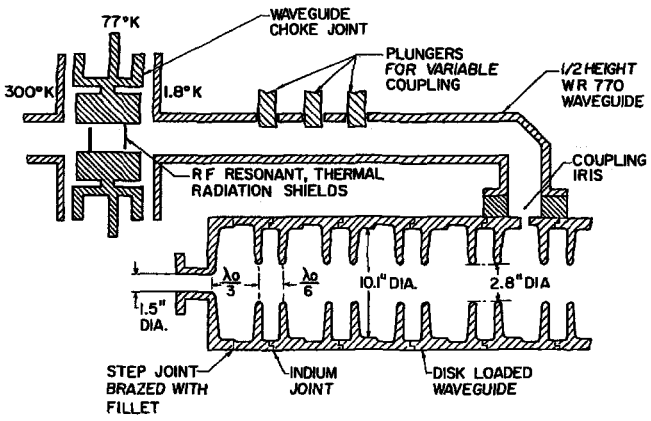

Fig. 1. Diagram of the 19 Cell Bi-periodic Accelerating Structure with RF Input System.

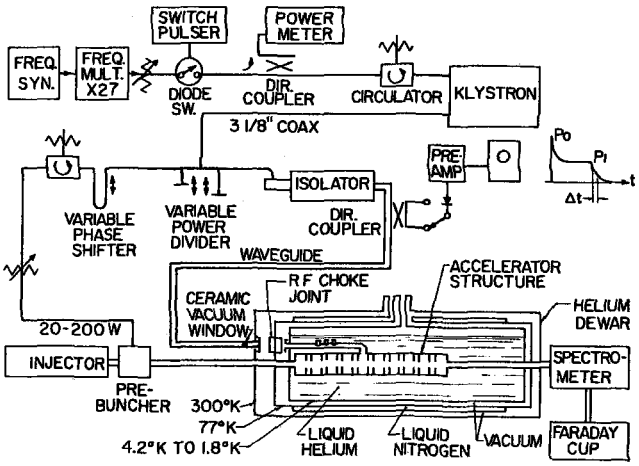

Fig. 2. Block diagram of RF and Cryogenic Components for the Five Foot 952 MHz Superconducting Linear Accelerator.

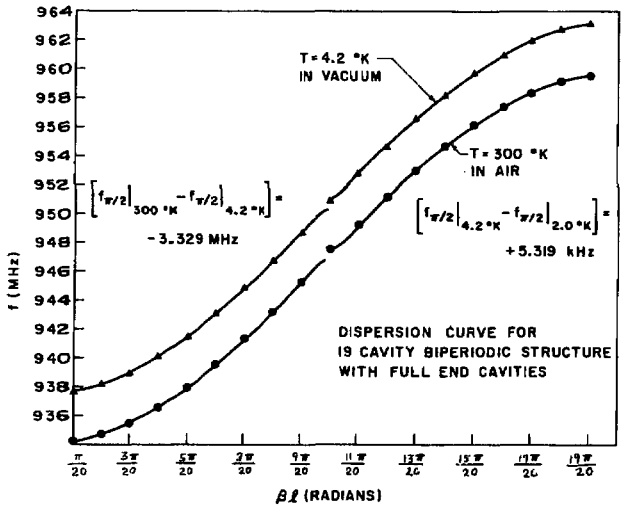

Fig. 3. Dispersion diagram for the 19 Cell Structure at 300°K and 4.2°K.

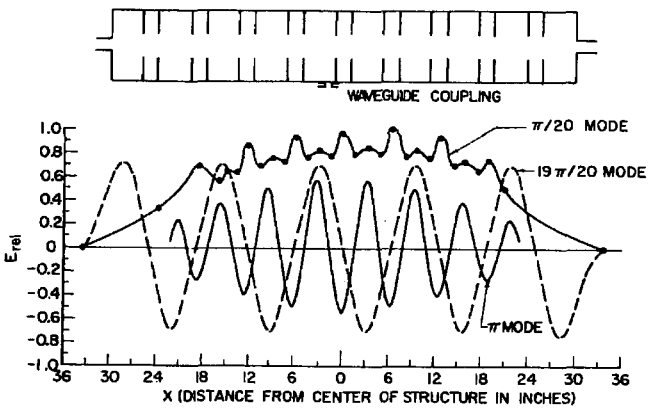

Fig. 4. Axial Field Profiles for the 19 Cell Bi-periodic Structure.

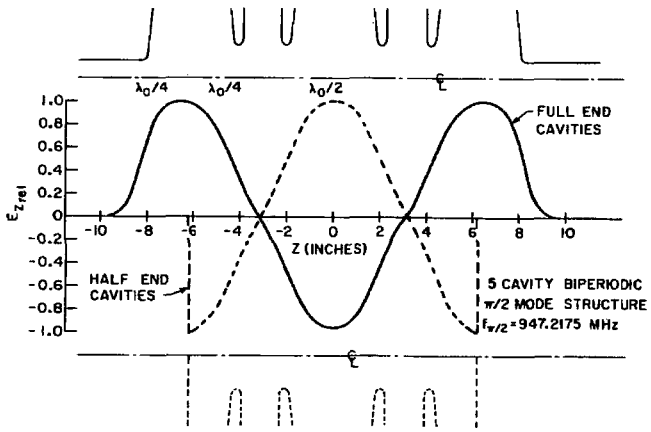

Fig. 5. Axial Field Profiles for the 5 Cell Bi-periodic Structure.